Chinese Chemical Letters 35 (2024) 109063

Contents lists available at ScienceDirect

Chinese Chemical Letters

journal homepage: www.elsevier.com/locate/cclet

Producing circularly polarized luminescence by radiative energy transfer from achiral metal-organic cage to chiral organic molecules

Zhao-Xia Lian[a], Xue-Zhi Wang[a], Chuang-Wei Zhou[a], Jiayu Li[b], Ming-De Li[b], Xiao-Ping Zhou[a,*], Dan Li[a]

[a] College of Chemistry and Materials Science, Guangdong Provincial Key Laboratory of Functional Supramolecular Coordination Materials and Applications, Jinan University, Guangzhou 510632, China
[b] College of Chemistry and Chemical Engineering, Key Laboratory for Preparation and Application of Ordered Structural Materials of Guangdong Province, Shantou University, Shantou 515063, China

ARTICLE INFO

Article history:
Received 1 August 2023
Revised 21 August 2023
Accepted 7 September 2023
Available online 9 September 2023

Keywords:
Circularly polarized luminescence
Metal-organic cage
Radiative energy transfer
Chiral small molecules
Bodipy
Chirality

ABSTRACT

The development of circularly polarized luminescence (CPL) materials with high performance is significantly important. Herein, we develop a facial strategy for fabricating a CPL-active system by employing an achiral luminescent metal-organic cage (MOC) and chiral boron dipyrromethene (BODIPY) molecules. CPL is achieved by taking advantage of the radiative energy transfer process, in which BODIPY molecules act as energy acceptors and MOCs act as donors. The CPL performance (maximum luminescence dissymmetry factor up to $\pm 1.5\times10^{-3}$) can be tuned by adjusting the ratio between MOCs and BODIPY. White-light emission with the CPL feature is obtained by using a ternary system including MOC, chiral BODIPY, and Rhodamine B. The present work provides a facile and universal strategy to construct a CPL-active system by integrating achiral luminophores and chiral molecules.

Circularly polarized luminescence (CPL) has attracted the increasing attention of scientists owing to its potential applications in a wide range of fields, including 3D displays [1], optical information storage [2], chiroptical sensors [3], and optoelectronic devices [4,5]. The construction of a circularly polarized luminescent system is inseparable from the two elements of chirality and luminescence. Generally, the covalent combination of chiral moieties and luminophores is the most common design strategy to directly fabricate CPL-active materials, while tedious synthesis is often unavoidable [6]. Besides, multicomponent co-assembly systems can be established through non-covalent interactions [7] (such as hydrogen bonds, π–π stacking interactions, and electrostatic interactions) between achiral luminophores and chiral components, in which achiral luminophores are endowed with CPL by chirality transfer [8]. In these multicomponent systems, one of the greatest merits is to reduce the synthesis difficulty of complex chiral systems. Meanwhile, intermolecular energy-transfer approaches including Förster resonance energy transfer (FRET) [9] and photon upconversion (UC) [10] have been reported in polymers [11], gels [12], liquid crystals [13], and metal-organic materials [14], which are confirmed to be effective in amplifying and modulating CPL. Although the preparation of CPL materials has made considerable progress to date, it is still of great significance and challenge to develop new CPL materials through simple methods.

Metal-organic cages (MOCs) are endowed with tunable functionalities through coordination-driven self-assembly of rationally designed organic ligands and selected metal ions. Owing to their well-defined cavities and great molecular dispersibility, MOCs have played an important role in the fields of molecular recognition and separation [15,16], catalysis [17–20], biomedicine [21], *etc*. For instance, MOCs can be used as a research platform to construct supramolecular photoluminescent materials derived from rigid aromatic organic ligands or lanthanides luminophores [22]. With the increasing demand for chiral functional materials, some CPL-MOCs have also been reported in the recent literature [23,24]. Wong and Law *et al*. developed the first CPL-active lanthanide cage by self-assembly of chiral ligands and europium (Eu) [25]. Thereafter, Yan *et al*. synthesized a Eu_4L_4 cage with CPL property *via* a chiral ancillary ligand induction strategy [26]. Besides, Qiu and Zhu *et al*. found that the twisted chiral MOC obtained by the coordination of chiral luminescent helicene ligands with zinc ions can emit CPL [27]. Clever *et al*. employed a shape-complementary assembly strategy of chiral ligand and achiral luminescent ligand to construct two cases of heteroleptic CPL-MOCs [28,29]. Furthermore, the CPL of MOCs has been triggered by host–guest approach. Sun *et al*. re-

* Corresponding author.
E-mail address: zhouxp@jnu.edu.cn (X.-P. Zhou).

https://doi.org/10.1016/j.cclet.2023.109063
1001-8417/

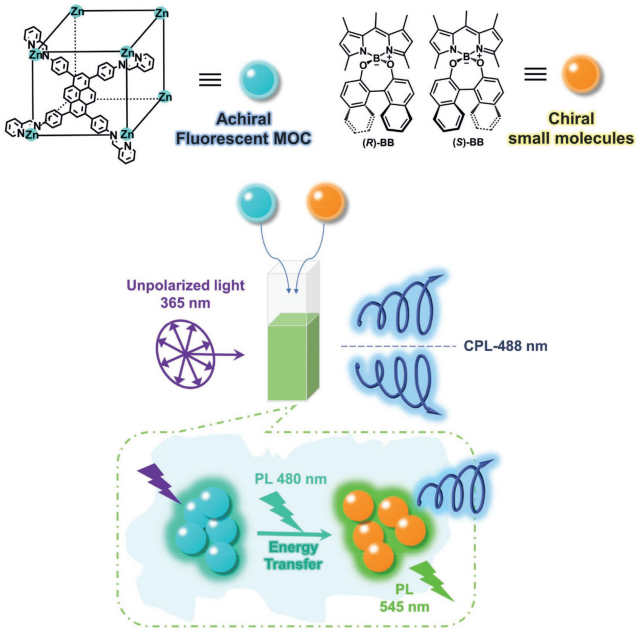

Scheme 1. Schematic illustration for CPL generation in the system of **1** and (*R*/*S*)-BB.

alized that lanthanide−organic cages through chiral induction of chiral guests successfully displayed CPL [30]. Liu *et al.* used chiral hexahedral cages to encapsulate dyes to achieve CPL [31]. Moreover, we reported the introduction of functional groups by post-synthetic modification (PSM) is an efficient strategy for MOCs to induce CPL [32]. However, all of the above examples have limitations that require chirality transfer. The biggest challenge lies in relaying chiral information from chiral moieties to the entire MOCs and selectively forming a stereoisomeric structure. To overcome this difficulty, the fluorescence-selective absorption mechanism has been applied to constructing polymer-based CPL materials [33–35]. Inspired by related research, we hypothesize that a CPL-active system can be established based on energy transfer between luminescent MOCs and chiral organic molecules without chirality transfer.

Recently, we found that the pyrene-based luminescent hexahedral Zn_8L_6 cage exhibits spontaneous aggregation and time-dependent luminescence enhancement in diluted solutions. In this work, we report a simple CPL system based on the achiral Zn_8L_6 cage and chiral BINOL-substituted BODIPYs (denoted as (*R*)-BB and (*S*)-BB, respectively) by radiative energy transfer (Scheme 1). Due to the effective spectral overlap, (*R*/*S*)-BB can effectively absorb the fluorescence emission from the Zn_8L_6 cage through the process of radiative energy transfer, which is demonstrated by the pump-probe fs-transient absorption measurements. The value of the luminescence dissymmetry factor (g_{lum}) of the system is proportional to the concentration of (*R*/*S*)-BB with maximum g_{lum} up to $\pm 1.5\times10^{-3}$, which is consistent with the value of absorption dissymmetry factor (g_{abs}) of (*R*/*S*)-BB and with reverse signals. The CPL of the mixed system is yielded by the selective absorption of the right-handed or left-handed light, providing a useful strategy for producing CPL-active materials.

The enantiomers (*R*/*S*)-BB were successfully synthesized from commercially available 1,3,5,7,8-pentamethyl-F-BODIPY and enantiopure (*R*/*S*)−1,1′-bi-2-naphthol according to the reported method (see Supporting information for experimental details) [36]. The Zn_8L_6 cage (denoted as **1**) was synthesized by subcomponent self-assembly of Zn^{2+}, 1,3,6,8-tetra(4-aminophenyl)pyrene, and 2-formylpyridine according to our previous work (detail see Supporting information) [37].

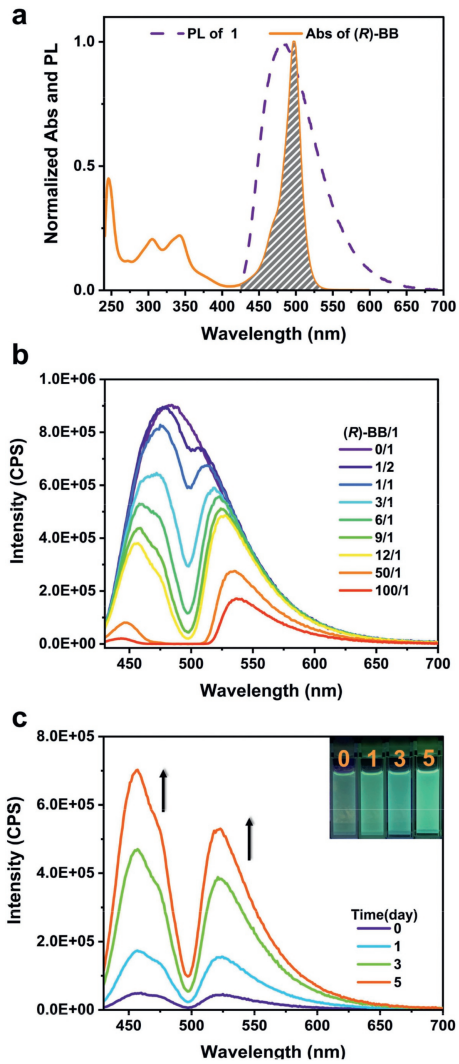

Fig. 1. (a) Normalized absorption (solid line) and emission (dashed line) of **1** (purple, $\lambda_{ex}=408$ nm) and (*R*)-BB (orange, $\lambda_{ex}=480$ nm) in CH_3OH/DMF (v/v=200/1). (b) Fluorescence emission spectrum of **1** with different molar fractions of (*R*)-BB (excited at 408 nm). (c) Time-dependent photoluminescent emission spectra of (*R*)-BB/**1**. Inset: photos of (*R*)-BB/**1** at different times under UV light (concentration of **1**=5.6×10^{-6} mol/L and (*R*)-BB = 5×10^{-5} mol/L).

Our previous study showed that **1** is an efficient and stable emitting material in a dilute solution after a period of incubation. Therefore, we employed the methanol solution of **1** after incubation for this investigation. **1** exhibits an abroad fluorescence band (from 425 nm to 675 nm) centered at around 480 nm in methanol. (*R*/*S*)-BB has a strong absorption band from 425 nm to 550 nm with a maximum of about 498 nm. As expected, the effective spectral overlap between the absorption spectrum of (*R*)-BB and the emission spectrum of **1** (Fig. 1a) was observed, indicating that an energy transfer process may occur between (*R*)-BB and **1**. We mixed the (*R*)-BB and **1** (denoted as (*R*)-BB/**1**) with different ratios in CH_3OH/DMF (v/v=200/1), and then measured their emission spectra. The emission intensity of **1** at 480 nm ($\lambda_{ex}=408$ nm) decreased significantly when the proportion of (*R*)-BB was increased (Fig. 1b). To further confirm intermolecular energy transfer between **1** and (*R*/*S*)-BB, we measured the emission spectra by using excitation light with different wavelengths. We excited (*R*)-BB using 480 nm due to the obvious absorbance of (*R*)-BB at 480 nm (Fig. S6 in Supporting information). Weak fluorescence was observed at 545 nm (photoluminescence quantum yield (PLQY) = 1%),

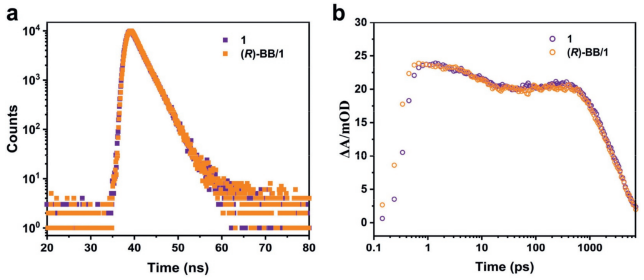

Fig. 2. (a) Fluorescence decay and (b) kinetic fitting of fs-Transient absorption spectra at 700 nm for pristine **1** and in the present of (*R*)-BB (concentration = 5×10^{-5} mol/L) in CH_3OH/DMF (v/v=200/1).

which showed obviously lower intensity than that of spectrum excited at 408 nm (Fig. S7 in Supporting information). These experiments show the occurrence of energy transfer between **1** and (*R/S*)-BB, which boosts the fluorescence of (*R/S*)-BB. Based on the time-dependent emission enhancement characteristic possessed by **1**, we also measured the time-dependent emission of (*R*)-BB/**1**. The luminescence at 545 nm of (*R*)-BB/**1** originating from (*R*)-BB can achieve synchronous growth within 5 days of incubation (Fig. 1c), further demonstrating the energy transfer between (*R*)-BB and **1**.

To gain insight into the energy transfer mechanism between **1** and (*R/S*)-BB, fluorescence decay profiles for pristine **1** and in the presence of (*R*)-BB were collected (Fig. 2a). The fluorescence lifetime of **1** remained unchanged after introducing (*R*)-BB. When the concentration of (*R*)-BB was 5×10^{-5} mol/L, the PLQY decreased from 73.4% to 18.6%. Given that the presence of (*R*)-BB only exhibits a reduction in PLQY without affecting the emissive lifetime, the energy transfer could not happen through FRET [38]. Additionally, any discernible spectral changes were not displayed in the UV−vis spectra of (*R*)-BB/**1** in comparison to pristine **1** and (*R*)-BB (Fig. S8 in Supporting information). The energy transfer mechanism is probably the process of radiative energy transfer. Furthermore, pump-probe fs-transient absorption measurements were carried out (Fig. S9 in Supporting information). The transient absorption peaks and kinetic traces of **1** at 700 nm were unchanged after the addition of (*R*)-BB (Fig. 2b). This result further corroborates the occurrence of radiative energy transfer between **1** and (*R*)-BB.

Subsequently, we sought to test whether cage **1** could form a host-guest with (*R/S*)-BB. Cage **1** dissolved in DMSO-d_6 with excess (*R*)-BB was characterized by NMR. As shown in ^{1}H NMR spectra (Fig. S10 in Supporting information), the peaks of (*R*)-BB/**1** do not show any shift as compared to the pristine **1** and (*R*)-BB, implying the absence of host-guest interaction. Moreover, the ^{1}H-^{1}H–diffusion ordered spectrum (DOSY, Fig. S11 in Supporting information) showed that all the peaks corresponding to **1** and (*R*)-BB had two sets of diffusion constants, demonstrating that there is no host-guest compound formed between them. Additionally, based on theoretical calculation, **1** contains a cavity volume of about 1115 Å^3 [37]. The molecular volume of (*R/S*)-BB is about 796 Å^3, which was calculated by using the accessible Connolly surface calculation of Materials Studio. The packing coefficient (the ratio between the guest volume and the host cavity volume) of (*R/S*)-BB for **1** is 71.4%. This value is too big regarding Rebek's 55% rule, further suggesting that **1** cannot encapsulate (*R/S*)-BB in the solution.

The chiroptical properties of (*R/S*)-BB/**1** were first evaluated by circular dichroism (CD) spectroscopy. The pristine chiral (*R/S*)-BB showed a significant Cotton effect. As illustrated by Fig. 3a, (*R*)-BB and (*S*)-BB show mirrored Cotton effects at 250, 340, and 498 nm, respectively. Although absorption (UV) increased sharply with achiral **1** addition, no corresponding new CD signals were present. The slightly decreasing CD signal intensity at 250 nm, is probably due to a strong competitive absorption at 250 nm of **1** (Fig. 3a). These results indicate that there is no ground-state chirality transfer between (*R/S*)-BB and cage **1**. Furthermore, the absorption dissymmetry factors (g_{abs}) of (*R/S*)-BB at 260, 332, and 498 nm were calculated to be 6.3×10^{-3}, 2.4×10^{-3}, and 1.0×10^{-3}, respectively (Fig. 3b).

The CPL of (*R/S*)-BB molecules were measured. We found that there was no obvious CPL signal presenting on their spectra (Fig. S12 in Supporting information). Interestingly, the CPL signals were observed in the (*R/S*)-BB/**1** (Fig. 3c). When increasing the proportion of (*R/S*)-BB, the intensity of the CPL signal increases gradually (Fig. 3d and Fig. S13 in Supporting information). This finding means that the magnitude of the luminescence dissymmetry factor g_{lum} value is determined by the concentration of chiral (*R/S*)-BB. Notably, the maximum g_{lum} value comes up to 1.5×10^{-3} (490 nm), which remains in the same order of magnitude as the value of g_{abs} (1.0×10^{-3}) at 498 nm. Moreover, we further found some correlations between CD and CPL spectra of (*R/S*)-BB/**1**. Specifically, (*R*)-BB shows a negative Cotton effect at around 498 nm while the CPL signal is positive. Conversely, (*S*)-BB displays a positive Cotton effect at around 498 nm, but the CPL sign is negative. At the same wavelength, the CPL signals are exactly opposite to the corresponding CD signals. Based on the above results, it can be speculated that the CPL was generated by chiral selective absorption of the fluorescence of **1**.

In order to verify the CPL generation mechanism more intuitively, CPL measurement experiments were performed by arranging the solutions of **1** and (*R/S*)-BB in independent sample cells. As illustrated in Fig. S14 (Supporting information), the separated system consists of two modes. In Mode 1, the sample cell of **1** is closer to the excitation source, followed by (*R/S*)-BB. Mirrored CPL signals with maximum emission around 490 nm were also observed in Fig. S14c, where **1** → (*R*)-BB showed a positive signal while **1** → (*S*)-BB showed a negative signal. These results were consistent with those from the mixture system of (*R/S*)-BB/**1** (Fig. 3c). The experiment of spatial separation manifests that CPL can be produced without any interaction. The mechanism is that the fluorescence of **1** partially absorbed by (*R/S*)-BB, making the amount of right-handed light and left-handed light is not equal. By contrast, when the position of **1** and (*R/S*)-BB was reversed in Mode 2, no CPL signal was observed (Figs. S14b and d). These results convincingly demonstrate that the chiral organic molecules (*R/S*)-BB can act like a molecular filter to yield CPL through the radiative energy transfer. When normal fluorescence of **1** interacts with (*R/S*)-BB, CPL will be generated. The CPL property can be evaluated by g_{lum} quantified as $g_{lum} = 2(I_L - I_R)/(I_L + I_R)$, where I_L and I_R are the intensities of the left- and right-handed CPL, respectively [39]. It should be noted that the unequal emission of the right-handed and left-handed light in the mixed system is caused by the selective absorption of the fluorescence of **1** by (*R/S*)-BB. Then, the absorption asymmetry factor g_{abs} is an important parameter reflecting the degree of difference in the absorption of left-handed and right-handed circularly polarized light by chiral molecules [23]. The g_{lum} value of the mixed system is determined by g_{abs} of (*R/S*)-BB.

For further studies, we synthesized another chiral *O*-BODIPY molecule (*R/S*)-BB2 (detail see Supporting information) by changing the substituent group to achieve new UV–vis absorption. UV–vis spectrum measurement showed that the absorption spectra corresponding to the BODIPY unit were located at 588 nm (Fig. S15 in Supporting information). The reduction of fluorescence emission of **1** certifies the occurrence of energy transfer from **1** to (*R/S*)-BB2 (Fig. S16 in Supporting information). The CD and CPL spectra of a mixture of **1** and (*R/S*)-BB2 were also measured (Figs. S17 and S18 in Supporting information). Similar to (*R/S*)-BB/**1**, the CPL emission wavelength is matched with the absorption peak at around 550 nm. Besides, the positive and negative CPL signals of (*R/S*)-BB2/**1**

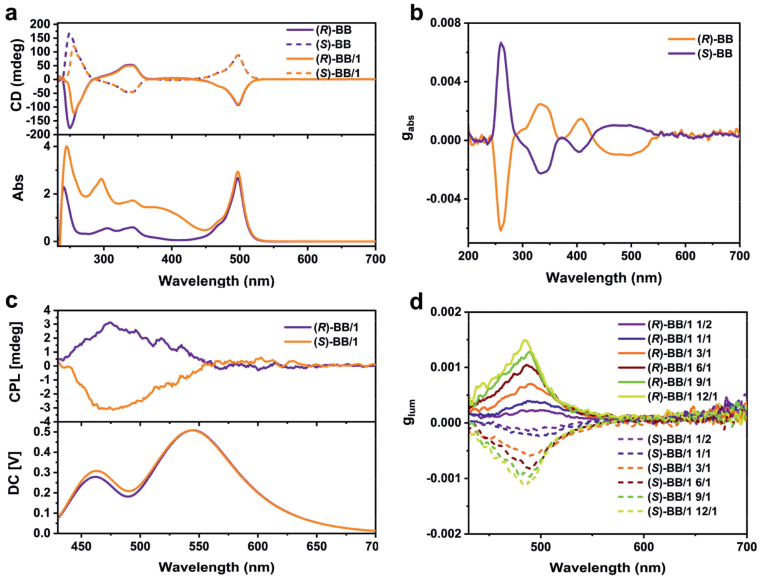

Fig. 3. (a) CD (top) and UV–vis spectra (bottom) of (*R*/*S*)-BB and (*R*/*S*)-BB/**1**. (b) Corresponding g_{abs} spectra of (*R*/*S*)-BB. (c) CPL spectra of (*R*/*S*)-BB/**1**. (d) Corresponding g_{lum} spectra in different molar fractions of (*R*/*S*)-BB in CH_3OH/DMF (v/v=200/1) solution of (*R*/*S*)-BB/**1** system (excited at 365 nm).

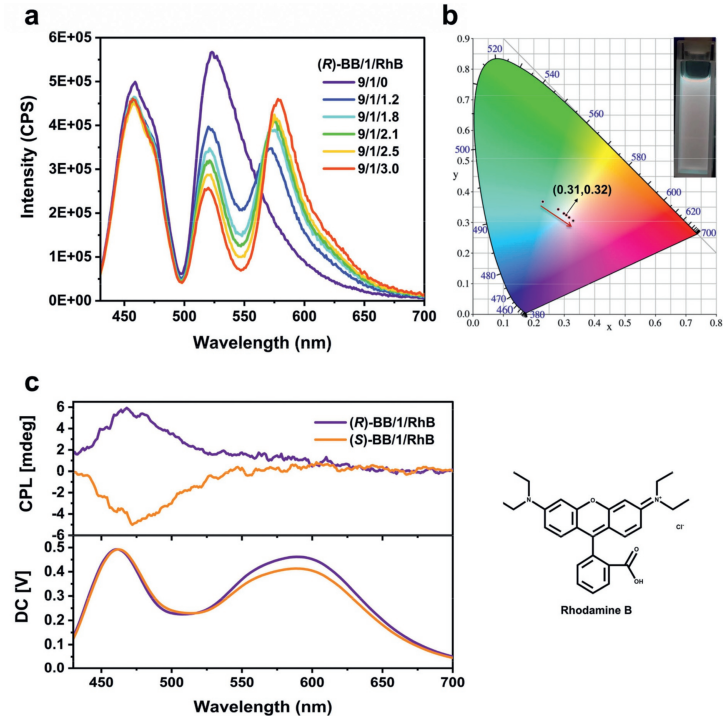

Fig. 4. (a) Fluorescence emission spectra and (b) the corresponding CIE 1931 chromaticity coordinates of (*R*)-BB/**1**/RhB. Inset: photograph under UV irradiation. (c) CPL of (*R*/*S*)-BB/**1**/RhB (concentration = 1.2×10^{-5} mol/L) in CH_3OH/DMF (v/v=200/1) and the chemical structure of Rhodamine B.

are also opposite to their CD signals at around 550 nm. These results demonstrated that tunable circularly polarized emission could be facile achieved by using this simple strategy.

White light-emitting materials are particularly important in lighting devices and display media. To achieve white emission, the red emission luminophore should be introduced into the system. The dye molecule Rhodamine B (RhB) emitting red light was selected. As shown in Fig. 4a, the emission spectrum of a mixture of (*R*)-BB, RhB, and **1** displayed three distinct bands, originating from the luminescence of **1**, (*R*)-BB, and RhB, respectively. Their intensities of emission bands can be tuned by changing the mixing ratio. When the concentration of RhB increases, the luminescence intensity of (*R*)-BB will decrease. This result indicated that an energy transfer process occurred between (*R*/*S*)-BB and RhB. Through a two-step sequential intermolecular energy transfer process, we successfully obtained a white-emitting solution using the mixture of 1/9/2.1 molar ratio of **1**, (*R*)-BB, and RhB, which could be confirmed by an inset fluorescence photo under 365 nm. As shown in Fig. 4b, its Commission Internationale de l'Éclairage (CIE) 1931 chromaticity diagram coordinate value is (0.31, 0.32), which is very close to the value of idea white light (0.33, 0.33). Moreover, the white emission was also CPL-active (Fig. 4c).

In summary, we have successfully developed a CPL-active system based on achiral luminescent MOC and chiral BODIPY molecules. Taking advantage of the optical activity of chiral BODIPY, normal fluorescence emitted by MOC is powerfully transformed into circularly polarized luminescence. The CPL signals can be regulated by the absorbance of chiral BODIPY molecules. White emission with the CPL feature is easily fabricated by introducing a red luminophore. This work provides a facile and useful strategy for the construction of CPL-active materials. We can predict that advanced luminescent materials with excellent CPL performance will be designed and prepared in the future by exploring this powerful strategy.

Declaration of competing interest

The authors declare that they have no known competing financial interests or personal relationships that could have appeared to influence the work reported in this paper.

Acknowledgments

This work was financially supported by the National Natural Science Foundation of China (Nos. 22171106, 21731002, 21975104, 21871172, and 22201101), the Guangdong Major Project of Basic and Applied Research (No. 2019B030302009), Guangdong Natural Science Foundation (No. 2022A1515011937), the Guangzhou Science and Technology Program (No. 202002030411), the China Postdoctoral Science Foundation (No. 2022M711327), Guangdong Basic and Applied Basic Research Foundation (No. 2022A1515110523), and Jinan University.

Supplementary materials

Supplementary material associated with this article can be found, in the online version, at doi:10.1016/j.cclet.2023.109063.

References

[1] M. Schadt, Annu. Rev. Mater. Sci. 27 (1997) 305–379.
[2] J.F. Sherson, H. Krauter, R.K. Olsson, et al., Nature 443 (2006) 557–560.
[3] R. Carr, N.H. Evans, D. Parker, Chem. Soc. Rev. 41 (2012) 7673–7686.
[4] Y. Yang, R.C. da Costa, M.J. Fuchter, et al., Nat. Photonics 7 (2013) 634–638.
[5] X. Zhang, Y. Zhang, H. Zhang, et al., Org. Lett. 21 (2019) 439–443.
[6] Y. Chen, Mater. Today Chem. 23 (2022) 100651.
[7] P. Xing, Y. Zhao, Acc. Chem. Res. 51 (2018) 2324–2334.
[8] C. Zhang, S. Li, X.Y. Dong, et al., Aggregate 2 (2021) e48.
[9] D. Yang, P. Duan, L. Zhang, et al., Nat. Commun. 8 (2017) 15727.
[10] D. Yang, J. Han, M. Liu, et al., Adv. Mater. 31 (2019) e1805683.
[11] Z. Wang, S. Liu, Y. Wang, et al., Macromol. Rapid Commun. 38 (2017) 1700150.
[12] C. Li, X. Jin, J. Han, et al., J. Phys. Chem. Lett. 12 (2021) 8566–8574.
[13] Y. Wu, M. Li, Z.G. Zheng, et al., J. Am. Chem. Soc. 145 (2023) 12951–12966.
[14] Z.L. Gong, Z.Q. Li, Y.W. Zhong, Aggregate 3 (2022) e177.
[15] D. Zhang, T.K. Ronson, Y.Q. Zou, et al., Nat. Rev. Chem. 5 (2021) 168–182.
[16] E.G. Percastegui, Chem. Commun. 58 (2022) 5055–5071.
[17] A.C. Ghosh, A. Legrand, R. Rajapaksha, et al., J. Am. Chem. Soc. 144 (2022) 3626–3636.
[18] Z. Zhang, Z. Zhao, Y. Hou, et al., Angew. Chem. Int. Ed. 58 (2019) 8862–8866.
[19] D. Li, X. Liu, L. Yang, et al., Chem. Sci. 14 (2023) 2237–2244.
[20] Y. Wang, J. Chen, J. Yang, et al., Angew. Chem. Int. Ed. 62 (2023) e202303288.
[21] C.Y. Zhu, M. Pan, C.Y. Su, Isr. J. Chem. 59 (2018) 209–219.
[22] J. Zhao, Z. Zhou, G. Li, et al., Natl. Sci. Rev. 8 (2021) nwab045.
[23] X.Y. Luo, M. Pan, Coord. Chem. Rev. 468 (2022) 214640.
[24] A. Zheng, T. Zhao, X. Jin, et al., Nanoscale 14 (2022) 1123–1135.
[25] C.T. Yeung, K.H. Yim, H.Y. Wong, et al., Nat. Commun. 8 (2017) 1128.
[26] Y. Zhou, H. Li, T. Zhu, et al., J. Am. Chem. Soc. 141 (2019) 19634–19643.
[27] Y.L. Ding, C.S. Shen, F.W. Gan, et al., Chin. Chem. Lett. 32 (2021) 3988–3992.
[28] K. Wu, J. Tessarolo, A. Baksi, et al., Angew. Chem. Int. Ed. 61 (2022) e202205725.
[29] J. Tessarolo, E. Benchimol, A. Jouaiti, et al., Chem. Commun. 59 (2023) 3467–3470.
[30] S.J. Hu, X.Q. Guo, L.P. Zhou, et al., J. Am. Chem. Soc. 144 (2022) 4244–4253.
[31] X.H. Tang, H. Jiang, Y.B. Si, et al., Chem 7 (2021) 2771–2786.
[32] D. Luo, Z.J. Yuan, L.J. Ping, et al., Angew. Chem. Int. Ed. 62 (2023) e202216977.
[33] B. Zhao, K. Pan, J. Deng, Macromolecules 52 (2018) 376–384.
[34] K. Yang, S. Ma, Y.P. Wu, et al., Chem. Mater. 35 (2023) 1273–1282.
[35] H. Zhong, B. Zhao, J.P. Deng, Adv. Opt. Mater. 11 (2023) 2202787.
[36] C. Tahtaoui, C. Thomas, F. Rohmer, et al., J. Org. Chem. 72 (2007) 269–272.
[37] D. Luo, L.X. Wu, Y. Zhang, et al., Sci China Chem. 65 (2022) 1105–1111.
[38] H. Sahoo, J. Photochem. Photobiol. C 12 (2011) 20–30.
[39] Z.L. Gong, X.F. Zhu, Z.H. Zhou, et al., Sci. China. Chem. 64 (2021) 2060–2104.